Topological superconductors and exact mobility edges in non-Hermitian quasicrystals

Zhen-Hua Wang,[1] Fuming Xu,[1] Lin Li,[2] Dong-Hui Xu,[3,*] and Bin Wang[1,†]
[1]*College of Physics and Optoelectronic Engineering, Shenzhen University, Shenzhen 518060, China*
[2]*College of Physics and Electronic Engineering, and Center for Computational Sciences, Sichuan Normal University, Chengdu 610068, China*
[3]*Department of Physics, Hubei University, Wuhan 430062, China*

(Received 17 August 2021; revised 20 December 2021; accepted 10 January 2022; published 20 January 2022)

We study a class of non-Hermitian topological superconductors described by one-dimensional Aubry-André Harper and mosaic quasiperiodic models with *p*-wave superconducting pairing, where the non-Hermiticity is introduced by on-site complex quasiperiodic potentials. We generalize two topological invariants, one is based on the transfer matrix method and the other is the generalized Majorana polarization, to characterize the topological superconducting phases and verify the existence of Majorana zero modes in non-Hermitian quasiperiodic superconductors. By combing the Lyapunov exponent, the fractional dimension of wave functions, and topological invariants, we investigate the localization phenomena, topological superconductivity, and topological phase transitions. In the non-Hermitian Aubry-André Harper model with *p*-wave pairing, the system undergoes an extended-critical-localized phase transition with increasing the complex phase. The localization transition is consistent with the topological phase transition and unconventional real-complex transition of eigenenergy. In the non-Hermitian mosaic model, we provide an analytical expression of mobility edges and prove the intrinsic relation between the mobility edges and unconventional real-complex transitions. Our discoveries unveil the richness of topological and localization phenomena in non-Hermitian quasicrystals with *p*-wave pairing.

DOI: 10.1103/PhysRevB.105.024514

I. INTRODUCTION

Topological phases have become one of the most fascinating and rapidly developing areas in condensed matter physics [1–4]. The topological phase is found in Hermitian systems, but has recently sparked tremendous interest in non-Hermitian systems. Non-Hermitian topological phases exhibit exotic phenomena, such as enriched topological classification [5–10], the breakdown of the conventional bulk-boundary correspondence [6,11–25], non-Hermitian skin effect [12,15,21,26–31], the appearance of topological phases with anomalous boundary modes [11,24,32–34], and non-Hermitian Majorana modes [7,26,35–44]. Most of existing studies have been focused on periodic lattices with translational invariance.

Recently, great interest has been devoted to studying the topological phases in non-Hermitian quasicrystals, where the interplay of topology, non-Hermiticity, and quasiperiodicity leads to rich interesting physical phenomena [45–60]. Quasicrystals constitute an intermediate phase between fully periodic lattices and fully disordered media, showing a long-range order but no periodicity. The Aubry-André Harper (AAH) model provides a paradigmatic example of a one-dimensional (1D) quasicrystal [61,62]. The non-Hermitian extensions of the AAH model produce exotic topological features. In particular, a non-Hermitian extension of the AAH Hamiltonian by complexification of the potential phase reveals that the localization phase transitions are of a topological nature and are characterized by winding numbers of energy spectra [57]. In a 1D nonreciprocal quasicrystal solely induced by the modulated asymmetric hopping amplitude, the topological phases with zero and nonzero energy edge modes are stable and can be characterized by the generalized Bott index [60,63]. The interplay between nonreciprocal hopping and complex quasiperiodic potentials gives rise to boundary-dependent self-dualities, and the asymmetrical Anderson localization is not necessarily in accordance with the topological phase transitions [64]. For a Su-Schrieffer-Heeger model with complex on-site potential, the delocalized, localized, and intermediate phases are further characterized by a pair of topological winding numbers [65]. Meanwhile, the non-Hermitian extensions of the AAH model present remarkable impacts of the (quasi)periodic on-site potentials on the $\mathcal{PT}$ symmetry breaking [51,52,54,55,66], butterfly spectrum [51,60], and mobility edges (MEs) [47,55,56,58,60,67–72]. On the other hand, the 1D non-Hermitian *p*-wave superconductor chain is another important paradigm in the topological community, and the interplay of disorder and topology deserves further investigation. The fate of Majorana zero modes (MZMs) and localization behaviors in non-Hermitian AAH models with *p*-wave pairing have been discussed recently [73–75]. However, the topological superconductivity and localization in other non-Hermitian quasiperiodic models have not been paid much attention, such as the quasiperiodic mosaic model [76] that hosts multiple MEs with the self-duality breaking. The MEs, which separate extended states from

*donghuixu@hubu.edu.cn
†binwang@szu.edu.cn

localized ones, induced by non-Hermiticity in the mosaic topological superconductors, (TSs) are less understood. It is unclear whether there is correspondence between the exact MEs and unconventional real-complex transition of eigenenergy. Furthermore, it is still worth studying whether there are some special topological invariants to describe the topological superconducting phase in non-Hermitian quasiperiodic TSs.

To address the above-mentioned issues, in this paper, we study the localization phenomena and topological phase transition in 1D AAH and mosaic models with p-wave superconducting pairing and complex on-site potentials, respectively. Two topological invariants, the $\mathcal{Z}_2$ topological invariant based on the transfer matrix method and the generalized Majorana polarization (MP), are generalized to characterize the topological superconducting phases and verify the existence of the MZMs. By using the energy spectrum, Lyapunov exponent (LE), the fractal dimensions of wave functions, and topological invariants, we characterize the localization and topological phase transitions. In the AAH model with p-wave pairing, the system undergoes an extended-critical-localized phase transition with increasing the complex phase. The localization transition is consistent with the topological phase transition and unconventional real-complex transition of eigenenergy. Meanwhile, the exponentially localized MZMs become more and more extended and then merge into the bulk. In the mosaic model with an even interval, the system always stays in the topological superconducting phase for arbitrary finite complex on-site potentials. We provide an analytical expression of MEs and prove the intrinsic relation between the MEs and unconventional real-complex transitions. In the mosaic model with an odd interval, localization phenomena, topological phase transitions, and rich MEs are induced. We cannot read out the localization transition from the change of the spectrum structure. Our analytical results are crucial to understanding the non-Hermitian MEs, unconventional real-complex transitions, and topological nature in non-Hermitian quasicrystals with p-wave pairing.

The rests of the paper is organized as follows. In Sec. II, the model Hamiltonians are introduced and two topological invariants are generalized to non-Hermitian quasicrystals. In Sec. III, we obtain the analytical expression of localization transition points and MEs by applying Avila's global theory. In Sec. IV A, the localization phase transition and topological phase diagram in non-Hermitian AAH models with p-wave superconducting pairing are studied. We also discuss the intrinsic relation between the localization transition and unconventional real-complex transitions. In Sec. IV B, the non-Hermitian mosaic models with p-wave pairing are investigated. We provide an analytical expression of non-Hermitian MEs and check whether there is correspondence between the MEs and unconventional real-complex transitions. In Sec. V, concluding remarks are given.

II. MODEL AND TOPOLOGICAL INVARIANTS

We consider a class of 1D quasiperiodic models with p-wave superconducting pairing which can be described by

$$H = \sum_{j=1}^{L-1}[-tc_{j+1}^{\dagger}c_j + \Delta c_{j+1}^{\dagger}c_j^{\dagger} + \text{H.c.}] + \sum_{j=1}^{L} V_j c_j^{\dagger}c_j, \quad (1)$$

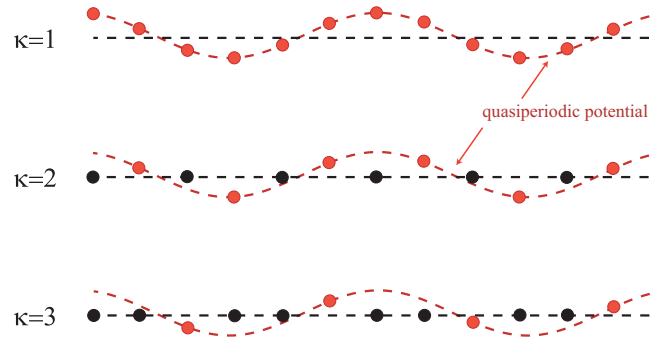

FIG. 1. The 1D quasiperiodic potentials of AAH ($\kappa = 1$) and mosaic ($\kappa = 2$ and 3) models. The red and black spheres denote the lattice sites whose potentials are quasiperiodic and zero, respectively, as shown by the corresponding red and black dashed lines.

with

$$V_j = \begin{cases} V_0 \cos[2\pi(\omega j + \theta)], & j = m\kappa \\ 0. & \text{otherwise,} \end{cases}$$

where $c_j^{\dagger}(c_j)$ is the creation (annihilation) operator of a spinless fermion at site j, t is the hopping amplitude and is set as the energy unit ($t = 1$), Δ is the p-wave superconducting pairing amplitude. V_j is the on-site complex quasiperiodic potential with the strength of $V_0 \equiv 2\lambda$ and the complex phase factor $\theta = \phi + ih$. h characterizes the non-Hermiticity of the system, and we will take it positive real. This paper is focused on the non-Hermitian effect, so we set $\phi = 0$ for convenience. ω is an irrational number characterizing the quasiperiodicity. It usually takes the value of the inverse of golden ratio [$\omega = (\sqrt{5} - 1)/2$], which can be approached by $\omega = \lim_{n\to\infty} F_{n-1}/F_n$, where F_n are the Fibonacci numbers defined recursively by $F_{n+1} = F_n + F_{n-1}$ with $F_0 = F_1 = 1$ [72,76–78]. Since the quasiperiodic potential periodically occurs with interval κ, we can define a quasicell with the nearest κ lattice sites. If the quasicell number is N, i.e., $m = 1, 2, \cdots, N$, then the system size becomes $L = \kappa N$. When $\Delta = 0$ and $\kappa = 1$, the model reduces to the non-Hermitian AAH model [57]. For $\kappa \geqslant 2$, the model is referred to as the non-Hermitian quasiperiodic mosaic model [72]. The quasiperiodic lattice models with $\kappa = 1$, 2, and 3 are pictorially shown in Fig. 1.

When $\kappa = 1$, $\Delta \neq 0$ and $h = 0$, the model in Eq. (1) describes a 1D Kitaev model with a real quasiperiodic potential, where the behavior of Majorana end modes and the localization of normal states have been studied recently [79–81]. When $h \neq 0$, the system corresponds to the non-Hermitian AAH model with p-wave pairing, and the interplay of non-Hermiticity and quasiperiodicity leads to an intriguing extended-critical-localized phase transition [73,75].

To characterize the non-Hermitian topological superconducting phases of the 1D quasiperiodic lattice with p-wave pairing, we make use of a $\mathcal{Z}_2$ topological invariant and the generalized MP. These two topological invariants work well in the Hermitian systems, and we would like to generalize to non-Hermitian cases. The generalization of topological invariants originally defined in Hermitian systems to non-Hermitian systems is an important issue since the topological invari-

ants in Hermitian systems cannot characterize the topological phases in non-Hermitian cases precisely.

First, we construct the $\mathcal{Z}_2$ topological invariant based on the transfer matrix that links topology to the eigenvalue structure of zero-energy end modes described by the Hamiltonian in Eq. (1) [79,81,82]. The Dirac fermion operator c_j can be expressed as the combination of two Majorana fermion operators $c_j = (a_j + ib_j)/2$, then the Hamiltonian in Eq. (1) is rewritten in terms of Majorana fermion operators as

$$H = \frac{i}{2}\sum_j [(-t+\Delta)a_j b_{j+1} + (t+\Delta)b_j a_{j+1} - V_j a_j b_j]. \tag{2}$$

Specifically, the Majorana end modes that decay into the bulk can be represented by the operators $Q_a = \sum_j \alpha_j a_j$, $Q_b = \sum_j \beta_j b_j$, where the wave functions $\alpha_j(\beta_j)$ obey the zero-energy equations of motion derived from Eq. (1). These equations can be represented in the transfer matrix forms [79,81,82]

$$\begin{pmatrix}\alpha_{j+1}\\ \alpha_j\end{pmatrix} = T_j\begin{pmatrix}\alpha_j\\ \alpha_{j-1}\end{pmatrix}, \text{where } T_j = \begin{pmatrix}\frac{V_j}{t+\Delta} & \frac{\Delta-t}{\Delta+t}\\ 1 & 0\end{pmatrix}, \tag{3}$$

$$\begin{pmatrix}\beta_{j+1}\\ \beta_j\end{pmatrix} = T'_j\begin{pmatrix}\beta_j\\ \beta_{j-1}\end{pmatrix}, \text{where } T'_j = \begin{pmatrix}\frac{V_j}{t-\Delta} & \frac{\Delta+t}{\Delta-t}\\ 1 & 0\end{pmatrix}. \tag{4}$$

T_j (T'_j) is the transfer matrix for the jth site. The existence of MZMs is determined by the eigenvalues of the transfer matrix of the whole lattice $T = \prod_{j=1}^{L} T_j$. Here T is a complex 2×2 matrix, therefore we cannot define a $\mathcal{Z}_2$ topological invariant based on the sign of Pfaffian to characterize the topological nature [79,81,82]. In the non-Hermitian system, both eigenvalues of T can still be calculated. Majorana modes bound to the ends of an infinite chain with open boundary conditions (OBCs) still require that both eigenvalues (A_1 and A_2) of T be either smaller or greater than unity in magnitude. For this situation, we define a topological invariant to characterize non-Hermitian topological superconducting phases, $\nu = -\mathrm{sgn}(\ln|A_1|\ln|A_2|) = -1$. If T has exactly one eigenvalue with a magnitude less than 1, the system is in the topologically trivial phase with no Majorana end modes, indicated by $\nu = 1$.

The MP is the other useful invariant to verify the existence of MZMs [83–88]. The generalized MP in non-Hermitian TSs has been studied in detail in Ref. [89]. Here, the particle-hole symmetry of our models obeys $H = -UH^TU^\dagger$ with $UU^\dagger = \pm I$. The two Majorana states are pinned at zero energy, but non-Hermiticity modifies their anticommutation relations. Different from Ref. [89], we use the left and right eigenstates to define the MP vector, $\langle\Psi^L|\mathcal{C}|\Psi^R\rangle$, where $|\Psi^{L(R)}\rangle$ represent the left (right) eigenstate in Nambu space, $\mathcal{C}$ is the particle-hole operator. In such a definition, the local structure of the MP is a ferromagnetic structure, which is consistent with the Hermitian limit [83,84]. All finite-energy eigenstates of the Hamiltonian in Eq. (1) satisfy $\langle\Psi^L|\mathcal{C}|\Psi^R\rangle = 0$ and Majorana states Φ satisfy $\langle\Phi^L|\mathcal{C}|\Phi^R\rangle = 1$. Additionally, in a region R_0 where such a Majorana state is localized, it must satisfy [83–89]

$$C = \frac{\left|\sum_{j\in R_0}\langle\Psi^L|\mathcal{C}_j|\Psi^R\rangle\right|}{\sum_{j\in R_0}\langle\Psi^R|\widehat{r}_j|\Psi^R\rangle} = 1, \tag{5}$$

where $\widehat{r}_j$ is the projection onto site j and $\mathcal{C}_j \equiv \mathcal{C}\widehat{r}_j$. The particle-hole operator $\mathcal{C} = e^{i\zeta}\tau^x\hat{\mathbf{K}}$ corresponds to the spinless systems. $\hat{\mathbf{K}}$ is a complex-conjugation operator, τ^y (σ^y) is the Pauli matrice in the particle-hole (spin) subspace, ζ is an arbitrary phase and can be chosen conveniently. When two Majorana modes are localized at opposite ends of the chain, one can simply set $R_0 = L/2$ in Eq. (1) with L the length of 1D quasiperiodic lattices.

III. LOCALIZATION AND CRITICAL PHASE

When p-wave pairing $\Delta \neq 0$, we can transform the disordered p-wave superconductor model to a disordered normal state model, and the transfer matrix method can still be used to determine the Anderson localization properties [73,79,80]. By performing a similarity transformation to the transfer matrix Eq. (3) as $T_j = \sqrt{\xi}S\tilde{T}_jS^{-1}$ with $S = \mathrm{diag}(\xi^{1/4}, \xi^{-1/4})$ and $\xi = \frac{t-\Delta}{t+\Delta}$ [73,75,79]. The new transfer matrix $\tilde{T}_j$ is

$$\tilde{T}_j = \begin{pmatrix}\frac{V_j}{\sqrt{t^2-\Delta^2}} & -1\\ 1 & 0\end{pmatrix}. \tag{6}$$

Thus, the total transfer matrix $T \equiv \prod_{j=1}^{L} T_j$ becomes

$$T(V_0, h, \Delta) = \left(\sqrt{\frac{t-\Delta}{t+\Delta}}\right)^L S\tilde{T}S^{-1}. \tag{7}$$

By applying Avila's global theory of quasiperiodic Schröinger operators [90], the LE can be defined as [72,79,82,91]

$$\gamma = \lim_{L\to\infty}\frac{1}{L}\ln\|T\|, \tag{8}$$

where $\|T\|$ denotes the norm of the matrix T [90]. Substituting Eq. (6) into Eq. (7), and taking the logarithm of the eigenvalues of Eq. (7), we obtain the LE as [79,91]

$$\gamma(V_0, h, \Delta) = \gamma\left(\frac{V_0}{\sqrt{t^2-\Delta^2}}, h, 0\right) + 1/2\ln\left(\frac{t-\Delta}{t+\Delta}\right), \tag{9}$$

which determines the topological phase transition in the quasiperiodic lattice with p-wave pairing [73,75,79]. When $\gamma(V_0, h, \Delta) = 0$, there is a delocalization-localization transition regarding the Majorana wave function α.

In Eq. (9), $\gamma(V_0/\sqrt{t^2-\Delta^2}, h, 0)$ corresponds to the LE of the normal states [79], which can be calculated following Refs. [72,78]. According to Eq. (6), the transfer matrix in the non-Hermitian AAH and mosaic models can be written as

$$\tilde{T}_j^\kappa = \begin{bmatrix}E - \frac{2\lambda\cos(2\pi\omega\kappa m + ih)}{\sqrt{t^2-\Delta^2}} & -1\\ 1 & 0\end{bmatrix}\begin{pmatrix}E & -1\\ 1 & 0\end{pmatrix}^{\kappa-1}. \tag{10}$$

The $(\kappa-1)$th power of the matrix can be calculated by use of the similarity transformation:

$$\begin{pmatrix}E & -1\\ 1 & 0\end{pmatrix}^{\kappa-1} = \begin{pmatrix}a_\kappa & -a_{\kappa-1}\\ a_{\kappa-1} & -a_{\kappa-2}\end{pmatrix}, \tag{11}$$

with

$$a_\kappa = \frac{1}{\sqrt{E^2-4}}\left[\left(\frac{E+\sqrt{E^2-4}}{2}\right)^\kappa - \left(\frac{E-\sqrt{E^2-4}}{2}\right)^\kappa\right].$$

For the non-Hermitian AAH model, $\kappa = 1$, $a_0 = 0$, and $a_1 = 1$. In the large-h limit, we have

$$\tilde{T}_j^{\kappa} = e^{(2\pi\omega\kappa m)i+|h|}\begin{pmatrix} -\frac{\lambda}{\sqrt{t^2-\Delta^2}} & 0 \\ 0 & 0 \end{pmatrix} + o(1). \tag{12}$$

We obtain $\gamma(V_0/\sqrt{t^2-\Delta^2}, h, 0) = |h| + \ln|\lambda/\sqrt{t^2-\Delta^2}| + o(1)$ and substituting it into Eq. (9), the LE becomes

$$\gamma(V_0, h, \Delta) = |h| + \ln\left|\frac{\lambda}{\sqrt{t^2-\Delta^2}}\right| + 1/2\ln\left(\frac{t-\Delta}{t+\Delta}\right). \tag{13}$$

Let Eq. (13)=0, then the critical localization transition point is

$$h_c = -\ln\left|\frac{\lambda}{t+\Delta}\right|, \tag{14}$$

which means when $h > h_c$, the states become localized. Equation (14) can be used to predict the topological phase transition h_c in the 1D p-wave quasiperiodic TSs.

Similarly, regarding the Majorana wave function β, the transfer matrix Eq. (4) can be transformed into $T_j' = \sqrt{\xi'}S'\tilde{T}_j'S'^{-1}$ with $S' = \mathrm{diag}(\xi'^{1/4}, \xi'^{-1/4})$ and $\xi' = \frac{t+\Delta}{t-\Delta}$ [73,79]. Thus, we get the LE

$$\gamma'(V_0, h, \Delta) = |h'| + \ln\left|\frac{\lambda}{\sqrt{t^2-\Delta^2}}\right| + 1/2\ln\left(\frac{t+\Delta}{t-\Delta}\right), \tag{15}$$

and the critical localization transition point is

$$h_c' = -\ln\left|\frac{\lambda}{t-\Delta}\right|, \tag{16}$$

which means when $h' > h_c'$, the wave function β becomes localized.

When $\kappa = 2$, the Hamiltonian in Eq. (1) becomes the non-Hermitian quasiperiodic mosaic model with p-wave pairing. The MEs are also expected to appear [72,78,81,92,93]. By performing a similarity transformation to the transfer matrix,

$$\tilde{T}_j^{\kappa} \simeq e^{(2\pi\omega\kappa m)i+|h|}\begin{pmatrix} -\frac{\lambda}{\sqrt{t^2-\Delta^2}} & -1 \\ 1 & 0 \end{pmatrix}\begin{pmatrix} a_2 & -a_1 \\ -a_1 & 0 \end{pmatrix}, \tag{17}$$

where $a_2 = E$. Then the MEs are obtained approximately by

$$E_c = \left|\frac{t+\Delta}{\lambda e^{(|h|-\ln|t-\Delta|)}}\right|. \tag{18}$$

The eigenstates with energies $|E + i\epsilon| < E_c$ and $|E + i\epsilon| > E_c$ correspond to the extended states and localized states, respectively [71,72].

To get an intuitive understanding of the above analytical results, we investigate the fractal dimension of the wave function, which is given by $\Gamma = -\lim_{L\to\infty}[\ln(\mathrm{IPR})/\ln L]$ [78]. For any given normalized wave function, the inverse participation ratio (IPR) is defined as $\mathrm{IPR}(n) = \sum_{j=1}^{L}(|\mu_{n,j}|^4 + |\nu_{n,j}|^4)$, where L denotes the total number of sites, j is the site index, and $\mu_{n,j}$, $\nu_{n,j}$ are the two components of the nth eigenstate in Nambu space. It is known that $\Gamma \to 1$ for the extended states and $\Gamma \to 0$ for the localized states. To characterize the localization of the whole system, the mean inverse of the participation ratio (MIPR) is also defined, $\mathrm{MIPR} = \frac{1}{2L}\sum_{n=1}^{2L}\mathrm{IPR}(n)$. For the extended state, the MIPR is of the order $1/L$, whereas it approaches 1 for the localized state [73,75].

IV. RESULTS AND DISCUSSIONS

In this section, we will discuss the localization and topological phase transitions from the perspective of energy spectrum, the fractal dimension Γ, unconventional real-complex transition of eigenenergy, and topological invariants in the non-Hermitian AAH and mosaic models with p-wave superconducting pairing, respectively. The collaboration between the p-wave superconducting pairing and non-Hermitian quasiperiodic potential yields localization phenomena, topological phase transitions, and rich MEs which are very different from the standard AAH and mosaic models.

A. Non-Hermitian AAH model with p-wave pairing

We first study the topological and localization phase transition induced by the quasiperiodic potential amplitude λ in 1D AAH model ($\kappa = 1$) with p-wave pairing. As shown in Fig. 2(a), the absolute values of energy eigenvalue $|E|$ and the corresponding fractal dimension Γ are presented as the function of λ under OBCs for the parameters $\Delta = 0.5$, $h = 0.5$, and $L = 300$. With the increase of λ, the exponentially localized MZMs become more and more extended and finally merge into the bulk when $\lambda > (t+\Delta)e^{-h}$, which indicates a phase transition from a topological superconducting phase to a trivial phase. The transition point is about $\lambda_c = (t+\Delta)e^{-h}$. Meanwhile, the topological phase transition is accompanied with the localization of bulk states [see the fractal dimension Γ in Fig. 2(a)]. The fractal dimension Γ shows a sudden drop at λ_c and approaches 0. From the MIPR in Fig. 2(b), we find that there are two delocalized phases for the region $\lambda < \lambda_c$, i.e., the extended phase and the critical one [73,75]. The MIPR of the critical phase shows a plateau behavior, which is greater than that of the extended one and less than that of the localized one. The topological phase transition point is consistent with the critical-localized transition point, and the extended-critical phase transition point is at $\lambda_c' = (t-\Delta)e^{-h}$.

In Figs. 2(c)–2(f), we discuss the effect of complex phase h on the localization and topological phase transition for fixed quasiperiodic potential amplitudes. We first consider the extended phase with $\lambda = 0.25$, see Figs. 2(c)–2(d). With the increase of h, the system also experiences an extended-critical-localized phase transition, and the transition point is determined by Eqs. (14) and (16), respectively. Meanwhile, the system undergoes a topological superconducting phase to a trivial phase transition, and the exponentially localized MZMs become more and more extended and then merge into the bulk when $h > h_c$. Again, the topological phase transition point is consistent with the critical-localized transition point. For $\lambda = 0.5$, the system is in the critical phase initially, and a critical-localized phase transition occurs as h increases. The transition point is determined by Eq. (14). There is no extended phase in such case, but the localization transition is still accompanied by the topological phase transition.

The non-Hermitian TS model in Eq. (1) only preserves the particle-hole symmetry, and the $\mathcal{PT}$-symmetry is broken. Therefore, the unconventional real-complex transition of en-

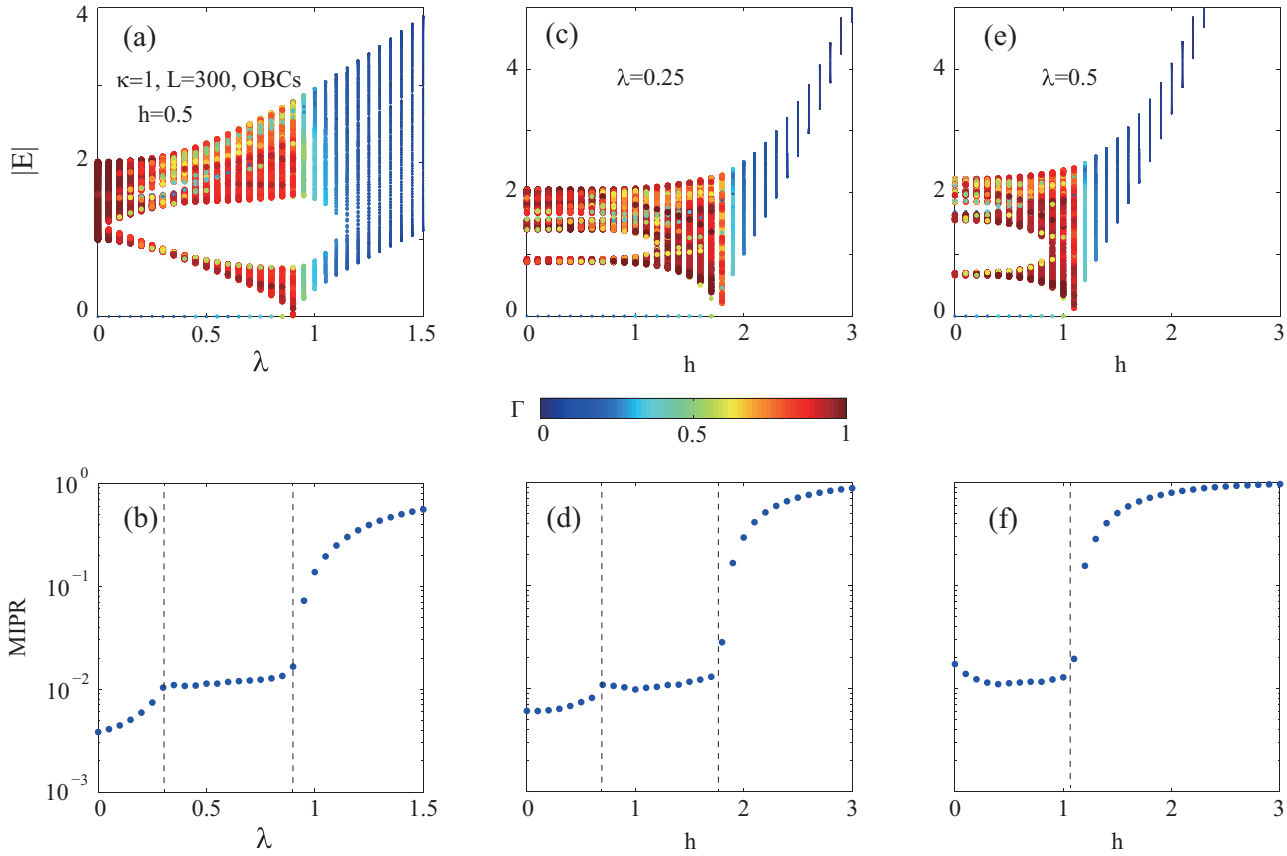

FIG. 2. The absolute values of eigenenergies $|E|$ and the corresponding fractal dimension Γ as a function of the strength of quasiperiodic potential λ (a) and complex phase h (b),(c) for $\kappa = 1$ under OBCs. The system size is $L = \kappa N = 300$. (d)–(f) The corresponding MIPR in (a)–(c). The dashed lines show the sharp increase of the MIPR at phase boundaries obtained by Eqs. (14) and (16).

ergy spectrum is expected to exist [73,74,94]. To study the real-complex transition of energy spectrum, periodic boundary conditions (PBCs) are used, which will avoid the edge effects. In Fig. 3, we take $\Delta = 0.5$, $L = 987$ and display the eigenenergies with various λ and h under PBCs. When $\lambda = 0.25$ and $h = 0.1$, the eigenenergies are completely real and the system is in the extended and topologically superconducting phase. When $\lambda = 0.25$, $h = 1$, and $\lambda = 0.5$, $h = 1$, the system is in the critical and topological superconducting phase, and the spectrum is complex with loops. If $\lambda = 0.25$ and $h = 2$, the system is in the localized and topologically trivial phase. There is a loop in the spectrum encircling the origin of the complex energy plane, which is absent when $h < h_c$. The loop encircling the origin causes a band inversion and a topological phase transition happens, where the system enters a topologically trivial phase without unpaired MZMs [73,75].

The topological superconducting phase in non-Hermitian TSs can also be characterized by two generalized topological invariants: the $\mathcal{Z}_2$ topological invariant based on transfer matrix and the generalized MP. To have a more comprehensive view of the topological nature and its connection with the localization property of states in 1D non-Hermitian TSs, we present the fractal dimension Γ of the bulk states, the $\mathcal{Z}_2$ topological invariant, zero-energy modes and the generalized MP in the parameter space spanned by λ and h in Fig. 4, respectively. For the fractal dimension Γ of the bulk states, we can calculate the Γ of the second smallest absolute value of the energy for convenient, which is always in the bulk state. Figure 4(a) shows the fractal dimension Γ of the bulk state as a function of λ and h. We find a region with $\Gamma \to 0$ (dark blue) in the $\lambda - h$ parameter space, which means that all the bulk states are localized. For the region $\Gamma \to 1$, all the states are extended or critical except the MZMs. Notably, the boundary (white dashed curve) of the delocalization-localization transition is determined by Eq. (14), $h_c = -\ln|\frac{\lambda}{t+\Delta}|$. In Fig. 4(b), the $\mathcal{Z}_2$ topological invariant $\nu = -1$ indicates the topological superconducting phase and $\nu = 1$ is the topologically trivial phase. The phase diagram obtained by the transfer matrix is the same as that obtained by the localization transition in Fig. 4(a). The boundary of the topological phase transition is consistent with that of the delocalization-localization transition. In Figs. 4(c)–4(d), we use the zero-energy end modes and the generalized MP to further verify the connection between the localization and topological phase transitions. The minimum values E_0 of $|E|$ are presented in the $\lambda - h$ parameter space. The region with $E_0 = 0$ means the existence of the MZMs, and $E_0 \neq 0$ corresponds to the topologically trivial phase. The MP C in Fig. 4(d) also confirm the above statements. The $\mathcal{Z}_2$ topological invariant and the generalized MP are therefore useful tools to characterize the topological superconducting phase in non-Hermitian quasiperiodic TSs.

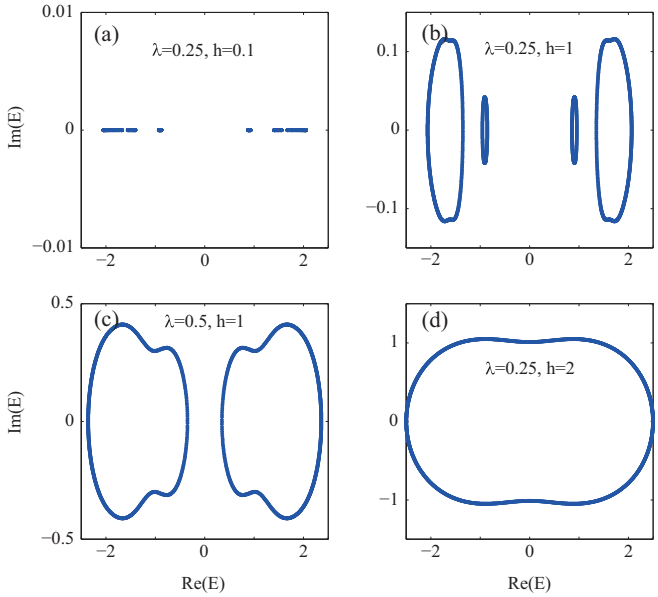

FIG. 3. The unconventional real-complex transition of eigenenergy under PBCs. Here we take $L = 987$ with negligible finite-size effects in numerical calculations. (a) $\lambda = 0.25$, $h = 0.1$ is taken from the extended and topologically superconducting phase. The eigenenergies are completely real. (b), (c) $\lambda = 0.25$, $h = 1$ and $\lambda = 0.5$, $h = 1$ are taken from the critical phase, the spectrum is complex with loops in the energy plane. (d) $\lambda = 0.25$, $h = 2$ is taken from the localized phase, a loop in the spectrum encircling the origin of the complex energy plane exists, which is absent in the topological superconducting phase.

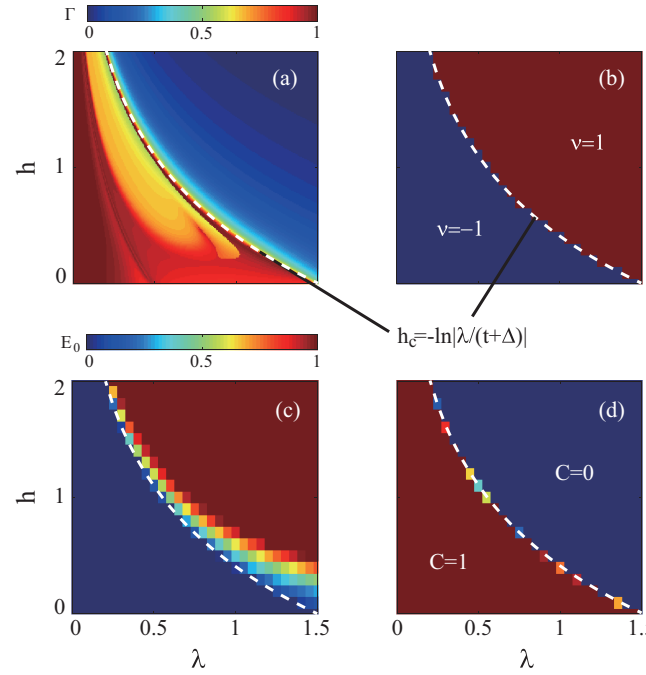

FIG. 4. The localization transition and its connection with the topological phase transition in the non-Hermitian AAH model ($\kappa = 1$) with $L = \kappa N = 300$ under OBCs. The white dashed curves correspond to the critical values $h_c = -\ln|\frac{\lambda}{t+\Delta}|$ in $\lambda - h$ plane. The p-wave pairing is $\Delta = 0.5$. (a) The fractal dimension Γ of the second smallest energy eigenvalue $|E|$, (b) the $\mathcal{Z}_2$ topological invariant ν based on the transfer matrix, (c) the minimum values E_0 of $|E|$, and (d) the generalized MP C as the function of the quasiperiodic potential amplitude λ and complex phase h.

B. Non-Hermitian mosaic model with *p*-wave pairing

When $\kappa \geqslant 2$, Eq. (1) describes the quasiperiodic mosaic model, which is highly significant to further explore the rich ME physics. Moreover, the MEs with analytic functional form can help in understanding the ME physics quantitatively and better investigate the effect of interacting effects on the MEs. In the following, we will study the exact MEs induced by the interplay between p-wave pairing and non-Hermitian quasiperiodic potential in the mosaic models.

Figure 5(a) shows the absolute values of eigenenergies and the corresponding fractal dimension Γ as the function of h under OBCs with the parameters $\Delta = \lambda = 0.5$ and $L = 600$. With the increase of h, a finite energy gap and a pair of zero-energy end states always exist, which indicates that the system is always in the topological superconducting phase. From the fractal dimension Γ of bulk states in Fig. 5(a), we can clearly see that the ME separates the extended and localized states. The numerical results of ME are consistent with the analytical expression in Eq. (18), indicating by the dashed line in Fig. 5(a). Γ approximately changes from one to zero when the energies across the dashed line. In Fig. 5(b), we depict the $\mathcal{Z}_2$ topological invariant based on transfer matrix and the generalized MP to check the topological nature of the non-Hermitian mosaic model with p-wave pairing. The $\nu = -1$ and $C = 1$ reveal that the system stays in the topological superconducting phase.

It is also found that correspondence between the exact MEs and unconventional real-complex transition of eigenenergy exists. In Fig. 5(c), we present the spectrum of the system under PBCs with fixed $h = 0.2$. For the extended states, the eigenenergies are completely real, as indicated in the dashed ellipses. For the localized states, the spectrum is complex with loops. In Fig. 5(d), $h = 0.8$, all the bulk states are localized, so the spectrum is complex with loops. Because the system is always in the topological superconducting phase, there is no loop in the spectrum encircling the origin of the complex energy plane [73,75].

In Fig. 5(e), we present the absolute value of eigenenergy $|E|$ and the corresponding fractal dimension Γ as the function of Δ with fixed $\lambda = h = 0.5$. With the increase of Δ, the MZMs become localized and then extended again. The bulk states still exhibit delocalization-localization transitions. When the eigenenergies across the dashed lines as shown in Fig. 5(e), Γ approximately changes from one to zero. Again, the numerical results of the MEs are consistent with the analytical curves obtained by Eq. (18). At the region around $\Delta = 1$, all the states are completely localized. In Fig. 5(f), we also present the imaginary parts of corresponding eigenenergies $|\mathrm{Im}(E)|$ as the function of $|E|$ and Δ. The exact MEs are identical to the boundary of the unconventional real-complex transition.

Figure 6 shows the behaviors for the mosaic model with $\kappa = 3$. In Fig. 6(a), $\Delta = 0$ is considered, and we show the absolute values of the eigenenergies and the corresponding

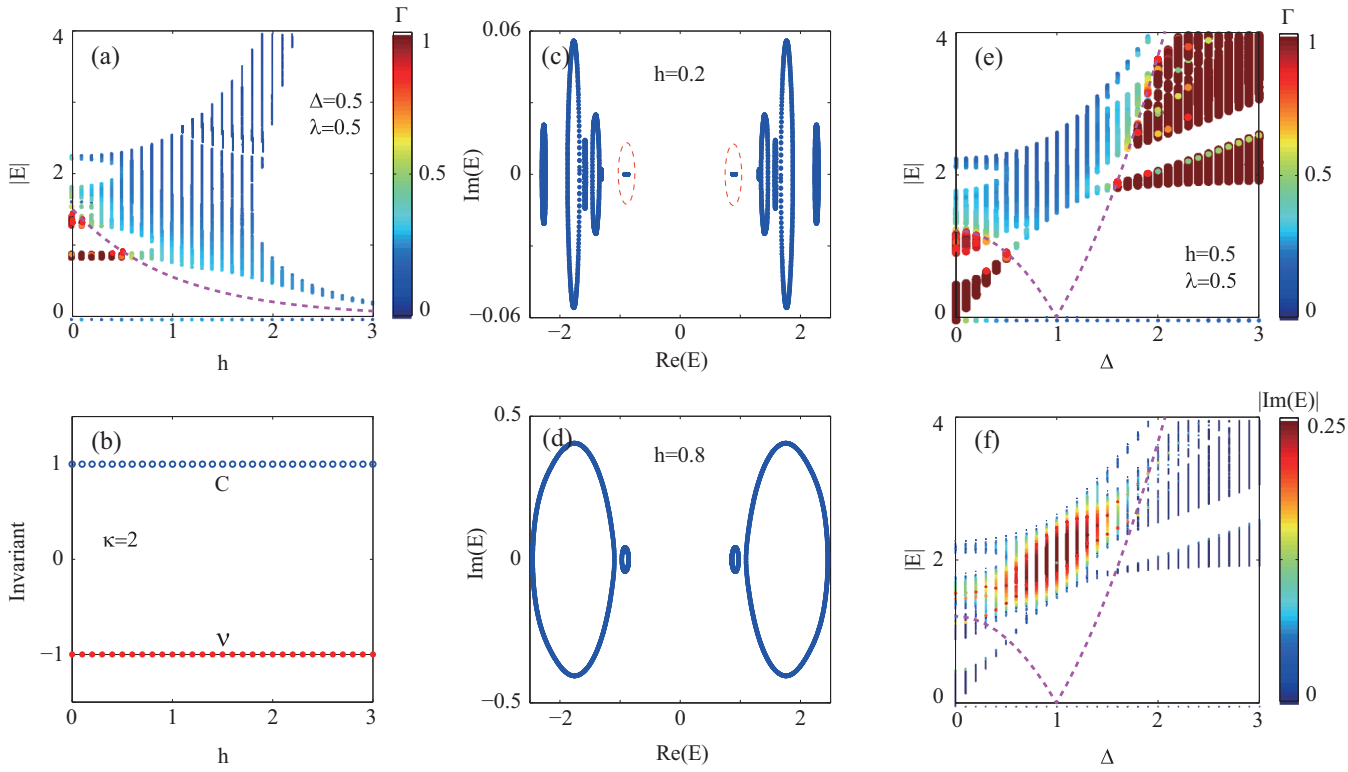

FIG. 5. (a) The absolute values of eigenenergies $|E|$ and the corresponding fractal dimension Γ as a function of the complex phase h for $\kappa = 2$ under OBCs. The dashed curve is the exact ME obtained from Eq. (18). (b) The two topological invariants $\nu = -1$ and $C = 1$ reveal that the system will always exist in the topological superconducting phase for any finite h. (c), (d) The eigenenergies of Eq. (1) with $L = \kappa N = 1974$ under PBCs. (e) The absolute values of eigenenergies, the fractal dimension Γ, and (f) imaginary parts $|\mathrm{Im}(E)|$ as the function of p-wave pairing Δ with $\lambda = h = 0.5$. The exact MEs are identical to the boundary of the unconventional real-complex transition.

fractal dimension Γ versus h with fixed $\lambda = 0.5$. The analytical expressions of the MEs are $|E_c| = (1 \pm \frac{1}{\lambda e^{|h|}})^{1/2}$, which are plotted as dashed lines. In Fig. 6(b), the p-wave pairing Δ is switched on. With the increase of h, the topological phase transition takes place, which can be verified by the $\mathcal{Z}_2$ topological invariant $\nu = -1$ and the generalized MP $C = 1$. The exponentially localized MZMs become more and more extended and then disappear into the bulk. Furthermore, the interplay between p-wave pairing and non-Hermitian quasiperiodic potential in the mosaic model can induce localization phenomena. The MEs separating the extended and localized states are very different from the standard mosaic model [76]. In this case, it's difficult to deduce the exact MEs from the transfer matrix method. According to the numerical results, we can introduce the following expressions to describe the MEs approximatively:

$$
\begin{aligned}
E_c^1 &= \left[1 - \ln\left|\frac{t-\Delta}{t+\Delta}\right| - \frac{1}{\lambda/(t+\Delta)}\frac{1}{e^{|h|-\ln|\frac{t-\Delta}{t+\Delta}|}}\right]^{1/2};\\
E_c^2 &= \left[1 - \ln\left|\frac{t-\Delta}{t+\Delta}\right| + \frac{1}{\lambda/(t+\Delta)}\frac{1}{e^{|h|-\ln|\frac{t-\Delta}{t+\Delta}|}}\right]^{1/2};\\
E_c^3 &= \left[1 + \ln|t-\Delta| - \frac{1}{\lambda/(t+\Delta)}\frac{1}{e^{|h|-\ln|2(t-\Delta)|}}\right]^{1/2};\\
E_c^4 &= \left[1 + \ln|t-\Delta| + \frac{1}{\lambda/(t+\Delta)}\frac{1}{e^{|h|+\ln|2(t-\Delta)|}}\right]^{1/2}. \qquad (19)
\end{aligned}
$$

When the eigenenergies across the dashed lines as shown in Fig. 6(b), Γ approximately changes from one to zero.

To check whether there is correspondence between the MEs and unconventional real-complex transition of eigenenergy, we take $\Delta = \lambda = 0.5$, $L = 987$, and display the eigenenergies of Eq. (1) with various h in Figs. 6(c)–6(f) under PBCs. When h is small, the eigenenergies close to $\mathrm{Re}(E) = 0$ are in the extended states, and the complex spectrum with loops are in the localized states. With the increase of $h = 0.7$, a complex spectrum with multiple loops is observed. Two pairs of loops are in the localized states and the other two pairs are in the extended states. Near the topological phase transition point, see Fig. 6(e), two loops encircling the origin of the complex energy plane are in the localized states and the other eigenenergies are in the extended states. In Fig. 6(f), the system enters into the topologically trivial phase. There is a large loop in the spectrum encircling the origin of the complex energy plane. The states in this large loop are localized, and the states in other small loops are still extended. In such a case, we cannot read out the localization transition from the change of the spectrum structure. The correspondence between the MEs and unconventional real-complex transition is broken.

V. CONCLUSIONS

In summary, we study the localization phenomena and topological phase transition in 1D AAH and mosaic quasiperiodic models with p-wave superconducting pairing and

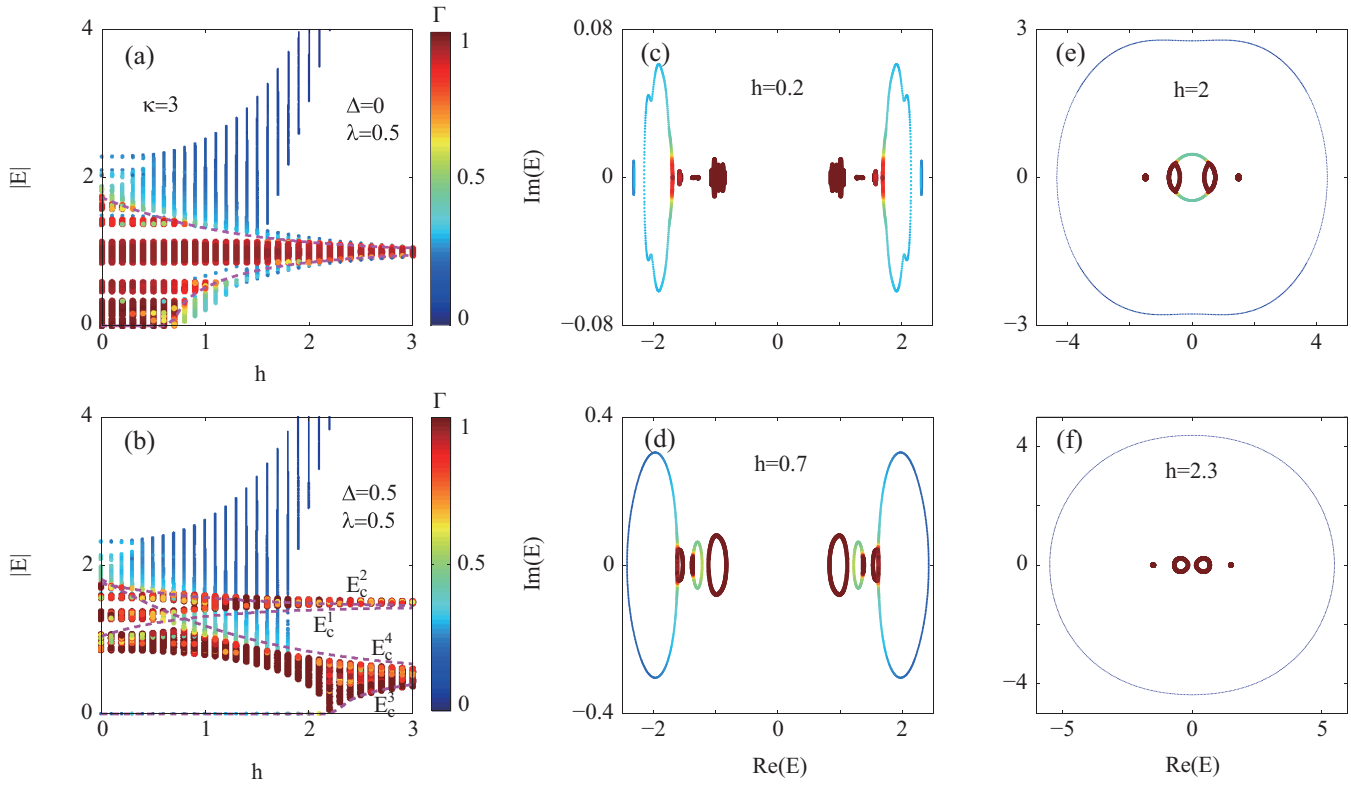

FIG. 6. (a) The absolute values of eigenenergies $|E|$ and the corresponding fractal dimension Γ as the function of complex phase h for $\kappa = 3$ with $\lambda = 0.5$ and $\Delta = 0$. The dashed curves are the exact MEs $|E_c| = (1 \pm \frac{1}{\lambda e^{|h|}})^{1/2}$. (b) $|E|$ and the fractal dimension Γ as the function of h for $\kappa = 3$ with $\lambda = \Delta = 0.5$. The dashed curves correspond to the MEs calculated by Eq. (19). The system is under OBCs and the size is $L = \kappa N = 987$. (c)–(f) The eigenenergies of the corresponding phase in Fig. 6(b) under PBCs.

complex on-site potentials, respectively. In such systems, we generalize two topological invariants, the $\mathcal{Z}_2$ topological invariant based on the transfer matrix, and the generalized MP, to characterize the topological superconducting phases. In non-Hermitian AAH quasicrystals with p-wave pairing, the system undergoes an extended-critical-localized phase transition with increasing the complex phase, and the critical-localized transition is accompanied by the topological phase transition. By analyzing the localization transition, the fractal dimensions of the states, and unconventional real-complex transition of eigenenergy, we prove the existence of the correspondence between the localization transition and unconventional real-complex transition. In mosaic models with even intervals, the system always stays in the topological superconducting phase for arbitrary finite complex on-site potentials. We provide analytical expression of MEs and prove the intrinsic relation between the MEs and unconventional real-complex transition. In the mosaic model with odd intervals, localization phenomena, topological phase transitions, and rich MEs are induced. The correspondence between the MEs and unconventional real-complex transitions is broken. We cannot read out the localization transition from the change of spectrum structure. In experiments, the models we studied can be simulated in photonic systems [95,96], where the on-site complex quasiperiodic potentials are introduced by the low-finesse intracavity etalon [57]. Recently, the Kitaev model was also simulated on quantum computers, which enabled the related quantum phenomenon to be physically realized [97–99]. Our study would be of importance and attractive for analytically exploring the richness of non-Hermitian localization phenomena and topological natures.

ACKNOWLEDGMENTS

This work was supported by the National Natural Science Foundation of China (Grants No. 11904234, No. 11774238, No. 12074108, No. 12174262, and No. 11704106). Z.-H.W., B.W., and F.X. also acknowledge support from the Shenzhen Natural Science Foundation (Grants No. JCYJ20190808151201649, No. JCYJ20190808150409413, and No. 20200812092737002). F.X. acknowledges support from the Natural Science Foundation of Guangdong Province (Grant No. 2020A1515011418). L.L. acknowledges support from the Project of Sichuan Science and Technology Program (Grant No. 2020YJ0136).

[1] M. Z. Hasan and C. L. Kane, Rev. Mod. Phys. **82**, 3045 (2010).
[2] X.-L. Qi and S.-C. Zhang, Rev. Mod. Phys. **83**, 1057 (2011).
[3] A. Bansil, H. Lin, and T. Das, Rev. Mod. Phys. **88**, 021004 (2016).

[4] N. P. Armitage, E. J. Mele, and A. Vishwanath, Rev. Mod. Phys. **90**, 015001 (2018).
[5] K. Kawabata, K. Shiozaki, M. Ueda, and M. Sato, Phys. Rev. X **9**, 041015 (2019).
[6] Z. Gong, Y. Ashida, K. Kawabata, K. Takasan, S. Higashikawa, and M. Ueda, Phys. Rev. X **8**, 031079 (2018).
[7] S. Lieu, Phys. Rev. B **100**, 085110 (2019).
[8] C.-H. Liu, H. Jiang, and S. Chen, Phys. Rev. B **99**, 125103 (2019).
[9] K. Kawabata, S. Higashikawa, Z. Gong, Y. Ashida, and M. Ueda, Nat. Commun. **10**, 297 (2019).
[10] L. Li, C. H. Lee, and J. Gong, Phys. Rev. B **100**, 075403 (2019).
[11] T. E. Lee, Phys. Rev. Lett. **116**, 133903 (2016).
[12] S. Yao and Z. Wang, Phys. Rev. Lett. **121**, 086803 (2018).
[13] S. Yao, F. Song, and Z. Wang, Phys. Rev. Lett. **121**, 136802 (2018).
[14] K. Yokomizo and S. Murakami, Phys. Rev. Lett. **123**, 066404 (2019).
[15] F. K. Kunst, E. Edvardsson, J. C. Budich, and E. J. Bergholtz, Phys. Rev. Lett. **121**, 026808 (2018).
[16] Y. Xiong, J. Phys. Commun. **2**, 035043 (2018).
[17] C. H. Lee and R. Thomale, Phys. Rev. B **99**, 201103(R) (2019).
[18] D. S. Borgnia, A. J. Kruchkov, and R.-J. Slager, Phys. Rev. Lett. **124**, 056802 (2020).
[19] V. M. Martinez Alvarez, J. E. Barrios Vargas, and L. E. F. Foa Torres, Phys. Rev. B **97**, 121401(R) (2018).
[20] S. Longhi, Phys. Rev. Res. **1**, 023013 (2019).
[21] E. J. Bergholtz, J. C. Budich, and F. K. Kunst, Rev. Mod. Phys. **93**, 015005 (2021).
[22] D. Leykam, K. Y. Bliokh, C. Huang, Y. D. Chong, and F. Nori, Phys. Rev. Lett. **118**, 040401 (2017).
[23] T.-S. Deng and W. Yi, Phys. Rev. B **100**, 035102 (2019).
[24] T. Liu, Y.-R. Zhang, Q. Ai, Z. Gong, K. Kawabata, M. Ueda, and F. Nori, Phys. Rev. Lett. **122**, 076801 (2019).
[25] S. Lieu, Phys. Rev. B **97**, 045106 (2018).
[26] A. McDonald, T. Pereg-Barnea, and A. A. Clerk, Phys. Rev. X **8**, 041031 (2018).
[27] V. M. Martinez Alvarez, J. E. Barrios Vargas, M. Berdakin, and L. E. F. Foa Torres, Eur. Phys. J.: Spec. Top. **227**, 1295 (2018).
[28] L. Xiao, T. Deng, K. Wang, G. Zhu, Z. Wang, W. Yi, and P. Xue, Nat. Phys. **16**, 761 (2020).
[29] F. Song, S. Yao, and Z. Wang, Phys. Rev. Lett. **123**, 246801 (2019).
[30] N. Okuma, K. Kawabata, K. Shiozaki, and M. Sato, Phys. Rev. Lett. **124**, 086801 (2020).
[31] K. Zhang, Z. Yang, and C. Fang, Phys. Rev. Lett. **125**, 126402 (2020).
[32] Y. Xu, S.-T. Wang, and L.-M. Duan, Phys. Rev. Lett. **118**, 045701 (2017).
[33] E. Edvardsson, F. K. Kunst, and E. J. Bergholtz, Phys. Rev. B **99**, 081302(R) (2019).
[34] X.-W. Luo and C. Zhang, Phys. Rev. Lett. **123**, 073601 (2019).
[35] K. Kawabata, Y. Ashida, H. Katsura, and M. Ueda, Phys. Rev. B **98**, 085116 (2018).
[36] C. Li, X. Z. Zhang, G. Zhang, and Z. Song, Phys. Rev. B **97**, 115436 (2018).
[37] M. van Caspel, S. E. T. Arze, and I. P. Castillo, SciPost Phys. **6**, 026 (2019).
[38] N. Okuma and M. Sato, Phys. Rev. Lett. **123**, 097701 (2019).
[39] N. Shibata and H. Katsura, Phys. Rev. B **99**, 174303 (2019).
[40] C. Yuce, Phys. Rev. A **93**, 062130 (2016).
[41] Q.-B. Zeng, B. Zhu, S. Chen, L. You, and R. Lü, Phys. Rev. A **94**, 022119 (2016).
[42] J. Avila, F. Penaranda, E. Prada, P. Sanjose, and R. Aguado, Commun. Phys. **2**, 133 (2019).
[43] P. San-Jose, J. Cayao, E. Prada, and R. Aguado, Sci. Rep. **6**, 21427 (2016).
[44] L. J. C. Li and Z. Song, Sci. Rep. **10**, 6807 (2020).
[45] N. Hatano and D. R. Nelson, Phys. Rev. Lett. **77**, 570 (1996).
[46] N. Hatano and D. R. Nelson, Phys. Rev. B **58**, 8384 (1998).
[47] A. Jazaeri and I. I. Satija, Phys. Rev. E **63**, 036222 (2001).
[48] J. Yamasaki and N. Hatano, Comput. Phys. Commun. **147**, 263 (2002).
[49] L. G. Molinari, J. Phys. A: Math. Theor. **42**, 265204 (2009).
[50] A. Basiri, Y. Bromberg, A. Yamilov, H. Cao, and T. Kottos, Phys. Rev. A **90**, 043815 (2014).
[51] C. Yuce, Phys. Lett. A **378**, 2024 (2014).
[52] C. H. Liang, D. D. Scott, and Y. N. Joglekar, Phys. Rev. A **89**, 030102(R) (2014).
[53] C. Mejía-Cortés and M. I. Molina, Phys. Rev. A **91**, 033815 (2015).
[54] A. K. Harter, T. E. Lee, and Y. N. Joglekar, Phys. Rev. A **93**, 062101 (2016).
[55] N. X. A. Rivolta, H. Benisty, and B. Maes, Phys. Rev. A **96**, 023864 (2017).
[56] Q.-B. Zeng, S. Chen, and R. Lü, Phys. Rev. A **95**, 062118 (2017).
[57] S. Longhi, Phys. Rev. Lett. **122**, 237601 (2019).
[58] S. Longhi, Opt. Lett. **44**, 1190 (2019).
[59] H. Jiang, L.-J. Lang, C. Yang, S.-L. Zhu, and S. Chen, Phys. Rev. B **100**, 054301 (2019).
[60] Q.-B. Zeng, Y.-B. Yang, and Y. Xu, Phys. Rev. B **101**, 020201(R) (2020).
[61] P. G. Harper, Proc. Phys. Soc. A **68**, 874 (1955).
[62] S. Aubry and G. André, Ann. Isr. Phys. Soc. **3**, 133 (1980).
[63] Q.-B. Zeng, Y.-B. Yang, and R. Lü, Phys. Rev. B **101**, 125418 (2020).
[64] X. Cai, Phys. Rev. B **103**, 014201 (2021).
[65] L. Zhou and W. Han, Chinese Phys. B **30**, 100308 (2021).
[66] S. Longhi, J. Phys. A: Math. Theor. **47**, 165302 (2014).
[67] S. Longhi, Phys. Rev. B **100**, 125157 (2019).
[68] Q.-B. Zeng and Y. Xu, Phys. Rev. Res. **2**, 033052 (2020).
[69] Y. Liu, X.-P. Jiang, J. Cao, and S. Chen, Phys. Rev. B **101**, 174205 (2020).
[70] T. Liu, H. Guo, Y. Pu, and S. Longhi, Phys. Rev. B **102**, 024205 (2020).
[71] Y. Liu, Y. Wang, Z. Zheng, and S. Chen, Phys. Rev. B **103**, 134208 (2021).
[72] Y. Liu, Y. Wang, X.-J. Liu, Q. Zhou, and S. Chen, Phys. Rev. B **103**, 014203 (2021).
[73] T. Liu, S. Cheng, H. Guo, and G. Xianlong, Phys. Rev. B **103**, 104203 (2021).
[74] S. Cheng and G. Xianlong, arXiv:2105.06621.
[75] X. Cai, Phys. Rev. B **103**, 214202 (2021).
[76] Y. Wang, L. Zhang, S. Niu, D. Yu, and X.-J. Liu, Phys. Rev. Lett. **125**, 073204 (2020).
[77] M. Kohmoto, Phys. Rev. Lett. **51**, 1198 (1983).
[78] Y. Wang, X. Xia, L. Zhang, H. Yao, S. Chen, J. You, Q. Zhou, and X.-J. Liu, Phys. Rev. Lett. **125**, 196604 (2020).

[79] W. DeGottardi, D. Sen, and S. Vishveshwara, Phys. Rev. Lett. **110**, 146404 (2013).
[80] X. Cai, L.-J. Lang, S. Chen, and Y. Wang, Phys. Rev. Lett. **110**, 176403 (2013).
[81] Q.-B. Zeng, R. Lü, and L. You, EPL **135**, 17003 (2021).
[82] W. DeGottardi, D. Sen, and S. Vishveshwara, New J. Phys. **13**, 065028 (2011).
[83] N. Sedlmayr and C. Bena, Phys. Rev. B **92**, 115115 (2015).
[84] N. Sedlmayr, J. M. Aguiar-Hualde, and C. Bena, Phys. Rev. B **93**, 155425 (2016).
[85] V. Kaladzhyan and C. Bena, SciPost Phys. **3**, 002 (2017).
[86] D. Sticlet, C. Bena, and P. Simon, Phys. Rev. Lett. **108**, 096802 (2012).
[87] N. Sedlmayr, V. Kaladzhyan, C. Dutreix, and C. Bena, Phys. Rev. B **96**, 184516 (2017).
[88] Z.-H. Wang, F. Xu, L. Li, R. Lü, B. Wang, and W.-Q. Chen, Phys. Rev. B **100**, 094531 (2019).
[89] Z.-H. Wang, F. Xu, L. Li, D.-H. Xu, W.-Q. Chen, and B. Wang, Phys. Rev. B **103**, 134507 (2021).
[90] A. Avila, Acta Math. **215**, 1 (2015).
[91] W. DeGottardi, M. Thakurathi, S. Vishveshwara, and D. Sen, Phys. Rev. B **88**, 165111 (2013).
[92] A. Duthie, S. Roy, and D. E. Logan, Phys. Rev. B **103**, L060201 (2021).
[93] T. Liu, X. Xia, S. Longhi, and L. Sanchez-Palencia, SciPost Phys. **12**, 027 (2022).
[94] Z.-H. Wang, F. Xu, L. Li, D.-H. Xu, and B. Wang, Phys. Rev. B **104**, 174501 (2021).
[95] J.-S. Xu, K. Sun, Y.-J. Han, C.-F. Li, J. K. Pachos, and G.-C. Guo, Nat. Commun. **7**, 13194 (2016).
[96] Z.-H. Liu, K. Sun, J. K. Pachos, M. Yang, Y. Meng, Y.-W. Liao, Q. Li, J.-F. Wang, Z.-Y. Luo, Y.-F. He, D.-Y. Huang, G.-R. Ding, J.-S. Xu, Y.-J. Han, C.-F. Li, and G.-C. Guo, PRX Quantum **2**, 030323 (2021).
[97] A. Smith, M. Kim, F. Pollmann, and J. Knolle, npj Quantum Inf. **5**, 106 (2019).
[98] O. E. Sommer, F. Piazza, and D. J. Luitz, Phys. Rev. Res. **3**, 023190 (2021).
[99] J. M. Koh, T. Tai, Y. H. Phee, W. E. Ng, and C. H. Lee, arXiv:2103.12783.